Author(s): Karppinen, Maarit & Yamauchi, H. & Fujinami, K. & Nakane, T. & Peitola, K. & Rundlöf, H. & Tellgren, R.

Title: Ca-substitution and O-doping effects in superconducting Cu(Ba0.8Sr0.2)2(Yb1-xCax)Cu2O6+z obtained from neutron diffraction refinements

Year: 1999

Version: Final published version

Please cite the original version:

Ca-substitution and O-doping effects in superconducting $Cu(Ba_{0.8}Sr_{0.2})_2(Yb_{1-x}Ca_x)Cu_2O_{6+z}$ obtained from neutron diffraction refinements

M. Karppinen

Materials and Structures Laboratory, Tokyo Institute of Technology, Yokohama 226-8503, Japan
and Laboratory of Inorganic and Analytical Chemistry, Helsinki University of Technology, FIN-02015 Espoo, Finland

H. Yamauchi, K. Fujinami, and T. Nakane

Materials and Structures Laboratory, Tokyo Institute of Technology, Yokohama 226-8503, Japan

K. Peitola

Laboratory of Inorganic and Analytical Chemistry, Helsinki University of Technology, FIN-02015 Espoo, Finland

H. Rundlöf and R. Tellgren

Inorganic Chemistry, Ångström Laboratory, Uppsala University, S-75121 Uppsala, Sweden
(Received 17 March 1998; revised manuscript received 13 October 1998)

Distinct calcium and oxygen doping effects were studied in the $Cu(Ba_{0.8}Sr_{0.2})_2(Yb_{1-x}Ca_x)Cu_2O_{6+z}$ (Cu-1212:P) system by means of neutron diffraction and superconducting quantum interference device experiments in the wide substitution ranges of $0 \leq x \leq 0.35$ and $0 < z < 1$. The effectiveness of the two different ways to introduce holes into the CuO_2 planes was compared both in respect to the capability to increase T_c and in terms of the hole production as estimated from neutron-diffraction data via bond-valence-sum calculation. Oxygen doping was found to increase the hole concentration less efficiently, and further, at a certain hole concentration value higher T_c values were obtained with calcium substitution than with oxygen doping. The two different hole-doping methods exhibited also different T_c vs Cu-O bond length relations. As a conclusion, the possible roles of the hole distribution in the in-plane Cu-O bond and the flatness of the CuO_2 planes in determining the superconducting properties were recognized. [S0163-1829(99)06929-5]

I. INTRODUCTION

The structures of superconducting cuprates are best described as members of different homologous series expressed by $M_mA_2Q_{n-1}Cu_nO_{m+2+2n\pm\delta}$ or $M\text{-}m2(n-1)n$. In these structures the superconductive $Q_{n-1}Cu_nO_{2n}$ ($Q=$Ca, rare-earth element R; $n=1-7$) ''infinite-layer'' blocks are sandwiched by AO ($A=$Sr, Ba, La) layers and $M_mO_{m\pm\delta}$ ($M=$e.g., Cu, Bi, Pb, Tl, Hg, C; $m=0-3$) ''charge reservoir'' blocks.[1] For understanding the phenomenon of high-T_c superconductivity, evaluation of the factors determining the superconducting properties is essential. The observed values of critical temperature T_c are believed to be related to the hole concentration in the CuO_2 planes, which is further commonly associated with, e.g., the valence of copper in the CuO_2 planes. An open challenge is, however, how to explicitly establish the values of such parameters.

In a common chemical approach the hole concentration in the CuO_2 planes is imagined as a mixed valence value of copper and estimated for the layered $M_mA_2Q_nCu_nO_{m+2+2n\pm\delta}$ cuprate structures by first analyzing the oxygen stoichiometry, i.e., δ in the $M_mO_{m\pm\delta}$ charge-reservoir block, and then sharing the observed excess oxidation evenly in between the different CuO_2 planes in the $Q_{n-1}Cu_nO_{2n}$ infinite-layer block to get a quantity which is best described as a ''nominal average copper valence'' or $V_{Cu,nom}$, i.e.,

$$V_{Cu,nom} \equiv 2 + [(2-C_{cr}) - 2C_{rs} + (n-1)(2-V_Q)]/n, \quad (1)$$

where C_{cr} and C_{rs} are the nominal charges of the $M_mO_{m\pm\delta}$ charge-reservoir block and the AO layer, respectively, and V_Q is the nominal integer oxidation number of the Q cation (e.g. $+$II for Ca and $+$III for Y) in the $Q_{n-1}Cu_nO_{2n}$ infinite-layer block.[2,3] The nominal charge of the $M_mO_{m\pm\delta}$ charge-reservoir block depends on the nominal valence of the metal constituent $M(V_{M,nom})$ and the oxygen stoichiometry δ, i.e., $C_{cr} = mV_{M,nom} - 2(m\pm\delta)$. On the other hand, the rocksalt-type spacing layers between the charge-reservoir and infinite-layer blocks are usually formed by formally neutral $A(+$II$)O$ units, i.e., $C_{rs}=0$.

Establishment of the oxygen stoichiometry by means of chemical analysis defines the actual hole concentration in an unambiguous way only in the simplest cases such as the $(La,Sr)_2CuO_{4\pm\delta}$ compound (i.e., 0201 phase). In the $CuBa_2RCu_2O_{7-\delta}$ structure (i.e., so-called ''123'' compound, or Cu-1212:P phase, where P stands for a perovskite-type charge-reservoir[1]), for example, even though the calculation of the average copper valence from the chemically analyzed oxygen content value is straightforward, the distribution of holes in between the $CuO_{1-\delta}$ chains (charge-reservoir block) and the CuO_2 planes (infinite-layer block) is nontrivial, and cannot be evaluated from the chemical analysis data.

Precise structural data obtained from neutron-diffraction experiments and the universal bond valence–bond length correlation, i.e., the concept of bond-valence-sum (BVS) as developed by Brown and Altermatt,[4,5] have been successfully utilized to establish the hole concentration vs δ behavior in
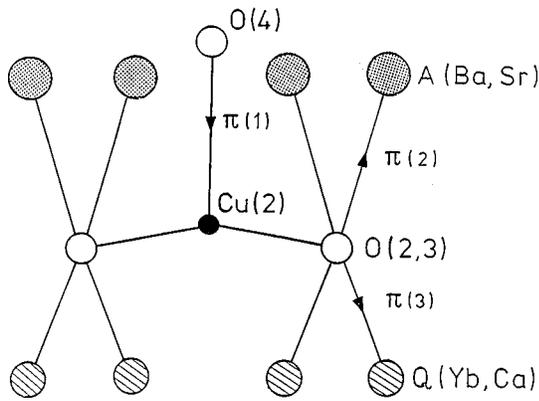
FIG. 1. The three hole-doping routes $\Pi(1)$, $\Pi(2)$, and $\Pi(3)$ for the pyramidal CuO_2 planes in layered $M_mA_2Q_{n-1}Cu_nO_{m+2+2n\pm\delta}$ cuprates and in the $Cu(1)(Ba,Sr)_2(Yb,Ca)Cu(2)_2O_{6+z}$ system.

the $CuBa_2YCu_2O_{7-\delta}$ compound.[6,7] Especially, when considering ''net holes'' which may reside either on copper or on oxygen in the CuO_2 planes rather than the valence of copper only, a parameter [i.e., $p(CuO_2)$, see Eq. (7)], which best explains the T_c vs δ relation in $CuBa_2YCu_2O_{7-\delta}$ is obtained.[8,9]

Another interesting question is, which are the optimum ways to fine tune the $p(CuO_2)$ parameter, i.e., to dope the existing as well as the ''not-yet-discovered'' cuprate superconductors to reach the ''universal maximum T_c.'' Based on the observation[10] that in the $p(CuO_2)$ value the contributions from the in-plane Cu-O bonds are counteracted and only the out-of-plane bonds from copper to the apical oxygen (O_{api}) and from the in-plane oxygen to the Q and A cations have net effects on the hole concentration, three different ways of doping the CuO_2 planes were defined in Refs. 2 and 3, i.e., (1) shortening the Cu-O_{api} bond and (2) lengthening the effective O-A or (3) O-Q bond in the $M_mA_2Q_{n-1}Cu_nO_{m+2+2n\pm\delta}$ structure (Fig. 1). It was also shown that these different doping routes may function either separately or in a collaborative manner. In the $CuBa_2(Y,Ca)Cu_2O_{7-\delta}$ system, for example, incorporation of oxygen into the $CuO_{1-\delta}$ chain is seen as gradual movements of O_{api} towards the CuO_2 plane [route (1)] and Ba away from the in-plane O atoms [route (2)] as the oxidation proceeds, while substitution of trivalent Y by divalent Ca introduces holes into the CuO_2 planes by lengthening the effective O-(Y, Ca) bond according to route (3).[2,3]

In order to clarify the distinctive features of the different doping routes and to study the efficiency of each route, e.g., in terms of hole production and the capability to increase T_c, the different doping routes should be facilitated separately in a fixed parent structure in wide doping ranges. The $CuA_2RCu_2O_{7-\delta}$ system is, in principle, a good model structure in which the joint effect of doping routes (1) and (2) achieved by oxygen doping can be compared to the structural changes associated with the Ca substitution, i.e., doping via route (3). However, when $A=Ba$ and $R=Y$, single phase samples are obtained only up to $x<0.20$.[11–13] Therefore, the $Cu(Ba_{0.8}Sr_{0.2})_2(Yb_{1-x}Ca_x)Cu_2O_{6+z}$ system, in which the solubility limit of Ca has been extended up to $x\approx0.40$,[14] was selected for the present systematic investigation of the Ca-substitution and O-doping effects. (Note that for the

amount of excess oxygen, z is used instead of ''$1-\delta$.'') In the following, essentially single-phase samples with $0<z<1$ and $0\leqslant x\leqslant0.35$ are dealt with. All the samples have been characterized by chemical analysis for the oxygen stoichiometry and by means of x-ray diffraction (XRD), neutron powder diffraction (NPD), and superconducting quantum interference device (SQUID) measurements for the structural and superconducting properties. For discussing the effects of the different hole-doping routes, the BVS calculation approach presented in detail in Refs. 2 and 3 and described shortly in Sec. II of the present contribution is utilized.

II. EXPERIMENTAL

Synthesis and characterization of the samples

Single-phase $Cu(Ba_{0.8}Sr_{0.2})_2(Yb_{1-x}Ca_x)Cu_2O_{6+z}$ powders with $x=0$, 0.10, 0.20, 0.25, and 0.35 were prepared from Yb_2O_3, $BaCO_3$, $SrCO_3$, $CaCO_3$, and CuO utilizing the technique developed and described in more detail in Ref. 14. In brief, stoichiometric mixtures of the starting materials were several times calcined and sintered (as pelletized) in air at 900–940 °C, and then oxidized in powder form by annealing in O_2 at 350–400 °C for 48 h. Oxygen-deficient Ca-free $Cu(Ba_{0.8}Sr_{0.2})_2YbCu_2O_{6+z}$ samples with varying oxygen content were obtained from the oxygenated $Cu(Ba_{0.8}Sr_{0.2})_2YbCu_2O_{6+z}$ ($z\approx0.96$) material by post-annealing in an Ar atmosphere at the following temperatures: 380 °C ($z\approx0.76$), 480 °C ($z\approx0.55$), 550 °C ($z\approx0.38$), 750 °C ($z\approx0.06$), 800 °C ($z\approx0$). The Ca-substituted oxygen-deficient ($z\approx0$) $Cu(Ba_{0.8}Sr_{0.2})_2(Yb_{1-x}Ca_x)Cu_2O_{6+z}$ samples were obtained from the corresponding oxygenated powders by annealing in Ar at 800 °C. In order to ensure the homogeneity of the oxygen content in the whole sample all these post-annealings were carried out in powder form in very small batches of ~150 mg in a thermobalance (MAC Science TG/DTA 2000 S) to be able to carefully control the temperature and atmosphere during the oxygen depletion and to *in situ* detect the changes in the weight/oxygen stoichiometry. In the thermogravimetric (TG) annealings the heating and cooling rates were 2 °C min⁻¹, and the isothermal heating period at the final temperatures was 6 h.

The level of excess oxygen in the samples was further confirmed by the coulometric Cu(+I)/Cu(+II) titration method[15] using the experimental setup described in Ref. 16. In this method, the possible trivalent copper and/or peroxide-type oxygen, i.e., α (CuO)$^+$, is reduced by Cu(+I) when dissolving the sample [expressed by $(Ba,Sr)_2(Yb_{1-x}Ca_x)(Cu(+III)_\alpha Cu(+I)_\beta)_3O_{6+z}$] in HCl solution containing a known excess (γ) of monovalent copper ions [Eq. (2)]. On the other hand, if the sample itself contains monovalent copper, i.e., β (CuO)$^-$, the Cu(+I) amount in the solution increases upon dissolving the sample [Eq. (3)]. Depending on the balance of α (CuO)$^+$ and β (CuO)$^-$ in the sample and the initial amount of monovalent copper (γ) in the solution, different quantities of electricity [$Q=(\gamma-\alpha+\beta)F$; $F=$Faraday constant] are detected when the coulometric back titration of the excess Cu(+I) is performed [Eq. (4)]. The average valence of copper ($V_{Cu}=2+\alpha-\beta$) and thus the oxygen excess ($z=0.5+0.5\alpha-0.5\beta-0.5x$) in

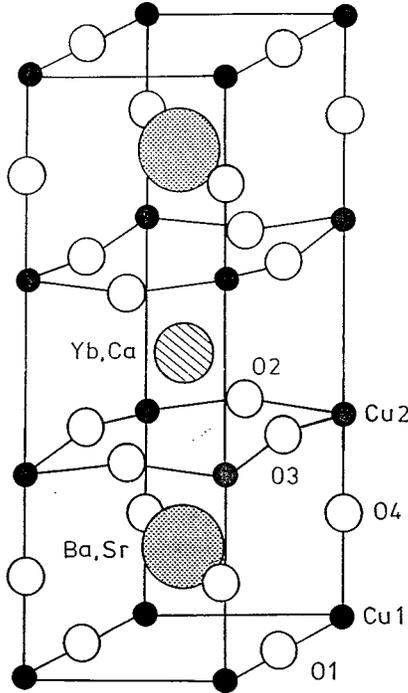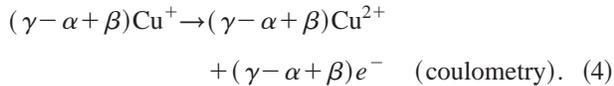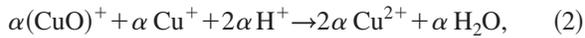FIG. 2. Schematic presentation of the $Cu(1)(Ba_{0.8}Sr_{0.2})_2(Yb_{1-x}Ca_x)Cu(2)_2O_{6+z}$ crystal structure and the present notation system for the atoms.

the sample exhibiting Cu valence values in the range of $+1 < V_{Cu} < +3$ can thus be calculated from the coulometric titration result:

$$\alpha(CuO)^+ + \alpha\, Cu^+ + 2\alpha\, H^+ \rightarrow 2\alpha\, Cu^{2+} + \alpha\, H_2O, \quad (2)$$

$$\beta(CuO)^- + 2\beta\, H^+ \rightarrow \beta\, Cu^+ + \beta\, H_2O, \quad (3)$$

$$(\gamma - \alpha + \beta)Cu^+ \rightarrow (\gamma - \alpha + \beta)Cu^{2+}$$
$$+ (\gamma - \alpha + \beta)e^- \quad \text{(coulometry).} \quad (4)$$

The synthesized samples were characterized for the phase purity and lattice parameters by an x-ray diffractometer (MAC Science MXP18VAHF;[22] Cu $K\alpha$ radiation), and for the superconducting properties by SQUID measurements (Quantum Design MPMS-5S) carried out down to 5 K in a field-cooling mode with a magnetic field of 10 Oe. The reported T_c values are onset temperatures of the diamagnetic signal.

Neutron-diffraction experiments

Neutron-diffraction experiments were carried out at the R2 reactor in Studsvik, Sweden. The neutron powder diffractometer consisting of a double Cu (220) monochromator system ($\lambda = 1.470\,\text{Å}$) and 35 ^{3}He detectors spaced 4.00° apart from each others, was used for the precise structure determination by scanning in steps of 0.08° over the 2θ range of 4.00–139.92°. The powder samples (each 2.5–4.0 g) were placed in vanadinium sample holders with a diameter of 6 mm, and the data were collected at 298 K. The neutron flux at the sample was approximately $10^6\,\text{cm}^{-2}\,\text{s}^{-1}$.

For the structure refinements a Rietveld program FULLPROF[17] was used. In Fig. 2, the unit cell of

$Cu(1)(Ba, Sr)_2(Yb, Ca)Cu(2)_2O_{6+z}$ is shown to illustrate the nomenclature of the atomic positions used in the present study. Since precise detection of very small gradual changes in the structure is crucial for the study, special care was taken to refine all data sets in a consistent way. The refinements were carried out supposing either the tetragonal $P4/mmm$ (No. 123) or the orthorhombic $Pmmm$ (No. 47) space group, and assuming a full occupancy for all the other atomic positions with the exception of the O(1) site. The cell parameters obtained from the XRD measurements were used as starting values for a, b, and c. Isotropic temperature factors were refined for all the atoms, except for O(1).

Bond-valence-sum (BVS) calculations

The bond-valence sums for the in-plane Cu(2), O(2), and O(3) atoms were calculated according to the scheme suggested by Brown and Altermatt,[4,5] i.e., first the bond valence s_{ij} of each i-j bond from an empirically determined parameter R_0 and from the experimental bond length R_{ij} (in Å) by

$$s_{ij} = \exp[(R_0 - R_{ij})/0.37], \quad (5)$$

and then the bond-valence sum around a species i by summing over the bond valences from all the nearest-neighboring counter ions, as

$$V_i = \pm \sum_j s_{ij}. \quad (6)$$

The calculated V_i sum was given as a positive value for the metal atoms and as a negative value for the oxygen atoms. The R_0 values[4,5] used in the present study are summarized in Table I. For the Cu-O bonds with copper in an intermediate valence state, the R_0 values were iterated in a self-consistent

TABLE I. Values for the parameter R_0 (Refs. 4 and 5) used in the present bond-valence calculations.

Bond	R_0 (Å)
Cu(+II)-O	1.679
Cu(+III)-O	1.730
Yb-O	1.965
Ca-O	1.967
Ba-O	2.285
Sr-O	2.118

TABLE II. Summary of the coulometric titration, NPD and SQUID results for the oxygen excess and T_c values in the $Cu(1)(Ba_{0.8}Sr_{0.2})_2(Yb_{1-x}Ca_x)Cu(2)_2O_{6+z}$ ($z \approx 0$) samples. The coulometric titration results are average values of at least five parallel analyses.

Ca content x nominal	Oxygen excess z, coulometry/NPD	T_c (K)
0.00	−0.03/0.225	<5
0.10	0.00/0.104	<5
0.20	0.00/0.166	<5
0.25	−0.02/0.072	27
0.35	−0.08/0.075	43

TABLE III. Summary of the coulometric titration, NPD and SQUID results for the oxygen excess and T_C values in the $Cu(1)(Ba_{0.8}Sr_{0.2})YbCu(2)_2O_{6+z}$ samples. The coulometric titration results are average values of at least five parallel analyses.

Oxygen excess z, coulometry/NPD	T_C (K)
−0.03/0.225	<5
0.06/0.201	<5
0.38/0.248	<5
0.55/0.350	37
0.76/0.817	55
0.96/0.999	82

way supposing that the value of R_0 depends linearly on the valence of Cu in between the limit values of 1.679 for Cu(+II) and 1.730 for Cu(+III).

The net hole concentration $p(CuO_2)$ in the CuO_2 planes was calculated as suggested by Tallon.[8]

$$p(CuO_2) = V_{Cu(2)} + V_{O(2)} + V_{O(3)} + 2. \qquad (7)$$

In order to distinguish the three different doping routes defined in Refs. 2 and 3, and discussed in the previous section, contributions from the Cu(2)-O(4), O(2,3)-(Ba, Sr), and O(2,3)-(Yb, Ca) bonds to the $p(CuO_2)$ value were separated according to Eqs. (8)–(11) into the partial hole concentrations $\Pi(1)$, $\Pi(2)$, and $\Pi(3)$:

$$p(CuO_2) \equiv \Pi(1) + \Pi(2) + \Pi(3), \qquad (8)$$

$$\Pi(1) \equiv s_{Cu(2)-O(4)}, \qquad (9)$$

$$\Pi(2) \equiv -2s_{O(2)-A} - 2s_{O(3)-A} + 1, \qquad (10)$$

$$\Pi(3) \equiv -2s_{O(2)-(R,Ca)} - 2s_{O(3)-(R,Ca)} + 1. \qquad (11)$$

Since the constant ''+2'' in Eq. (7) is shared just empirically between $\Pi(1)$, $\Pi(2)$, and $\Pi(3)$ [Eqs. (9)–(11)], it is obvious that not the absolute values but only the changes in these parameters are meaningful. Therefore, the $\Pi(1)$, $\Pi(2)$, $\Pi(3)$, and $p(CuO_2)$ values were standardized against an extrapolated ''zero sample'' with $x=0$ and $z=0$ to get the corresponding $\Delta\Pi(1)$, $\Delta\Pi(2)$, $\Delta\Pi(3)$, and $\Delta p(CuO_2)$ values.

III. RESULTS

Judging from the x-ray-diffraction data, the synthesized $Cu(Ba_{0.8}Sr_{0.2})_2(Yb_{1-x}Ca_x)Cu_2O_{6+z}$ samples were essentially of single-phase in the whole substitutional range of $0 \leq x \leq 0.35$ and $0 < z < 1$. Only in the XRD pattern of the Ca-free $Cu(Ba_{0.8}Sr_{0.2})_2YbCu_2O_{6+z}$ samples were traces of

TABLE IV. NPD refinement results for the $Cu(1)(Ba_{0.8}Sr_{0.2})_2(Yb_{1-x}Ca_x)Cu(2)_2O_{6+z}$ samples ($z \approx 0$) with $x=0.10$, 0.20, 0.25, and 0.35. Space group $P4/mmm$ (No. 123): Yb/Ca at (0.5, 0.5, 0.5), Ba/Sr at (0.5, 0.5, z), Cu(1) at (0, 0, 0), Cu(2) at (0, 0, z), O(1) at (0, 0.5, 0), O(2) at (0.5, 0, z), and O(4) at (0, 0, z).

x		0.10	0.20	0.25	0.35
a (in Å)		3.8314(2)	3.8272(2)	3.8320(2)	3.8334(2)
c (in Å)		11.745(1.0)	11.735(0.7)	11.736(0.8)	11.734(0.9)
Yb/Ca	n	0.90/0.10	0.80/0.20	0.75/0.25	0.65/0.35
	B (in Å²)	0.57	0.50	0.39	0.26
Ba/Sr	z	0.198 45(40)	0.197 89(30)	0.197 19(30)	0.197 55(30)
	n	0.8/0.2	0.8/0.2	0.8/0.2	0.8/0.2
	B (in Å²)	0.26	0.55	0.53	0.51
Cu(1)	B (in Å²)	1.00	1.13	1.06	1.19
Cu(2)	z	0.360 34(30)	0.360 47(20)	0.360 95(30)	0.361 35(30)
	B (in Å²)	0.30	0.10	0.13	0.13
O(1)	n	0.104	0.166	0.072	0.075
O(2)	z	0.380 61(30)	0.380 09(20)	0.378 88(20)	0.378 50(20)
	B (in Å²)	0.26	0.63	0.46	0.56
O(4)	z	0.155 95(60)	0.155 45(40)	0.153 77(50)	0.154 11(50)
	B (in Å²)	1.54	1.73	1.95	2.15
R_p (%)		3.94	4.41	3.54	3.67
R_{wp} (%)		5.37	6.29	4.84	5.06
χ^2		6.80	7.10	4.72	5.74
Bond lengths	Yb/Ca-O(2)	2.3741(×8)	2.3749	2.3857(×8)	2.3888(×8)
	Ba/Sr-O(1)	3.0171(×0.104)	3.0084(×0.166)	3.0045(×0.072)	3.0079(×0.075)
	-O(2)	2.8718(×4)	2.8688(×4)	2.8666(×4)	2.8605(×4)
	-O(4)	2.7548(×4)	2.7516(×4)	2.7571(×4)	2.7581(×4)
	Cu(1)-O(1)	1.9157(×2×0.104)	1.9134(×2×0.166)	1.9160(×2×0.072)	1.9167(×2×0.075)
	-O(4)	1.8317(×2)	1.8235(×2)	1.8047(×2)	1.8084(×2)
	Cu(2)-O(2)	1.9304(×4)	1.9274(×4)	1.9275(×4)	1.9272(×4)
	-O(4)	2.4006(×1)	2.4050(×1)	2.4315(×1)	2.4318(×1)

TABLE V. NPD refinement results for the Cu(1)(Ba$_{0.8}$Sr$_{0.2}$)$_2$YbCu(2)$_2$O$_{6+z}$ samples with $z_{coulom} = -0.03$, 0.06, 0.38, 0.55, 0.76, and 0.96. Space groups $P4/mmm$ (No. 123) and $Pmmm$ (No. 47): Yb/Ca at (0.5, 0.5, 0.5), Ba/Sr at (0.5, 0.5, z), Cu(1) at (0, 0, 0), Cu(2) at (0, 0, z), O(1) at (0, 0.5, 0), O(2) at (0.5, 0, z), O(3) at (0, 0.5, z), and O(4) at (0, 0, z).

z_{coulom}		−0.03	0.06	0.38	0.55	0.76	0.96
a (in Å)		3.8334(6)	3.8342(3)	3.8355(2)	3.8172(2)	3.8040(2)	3.7934(2)
b (in Å)					3.8465(2)	3.8583(2)	3.8615(2)
c (in Å)		11.736(2.0)	11.743(1.2)	11.718(0.7)	11.667(0.7)	11.637(0.8)	11.614(0.8)
Yb	B (in Å^2)	0.92	0.57	0.68	0.58	0.24	0.15
Ba/S	z	0.200 42(90)	0.198 41(50)	0.198 06(30)	0.193 07(30)	0.188 88(30)	0.184 17(30)
	n	0.8/0.2	0.8/0.2	0.8/0.2	0.8/0.2	0.8/0.2	0.8/0.2
	B (in Å^2)	0.30	0.17	0.37	0.49	0.38	0.58
Cu(1)	B (in Å^2)	1.80	0.92	0.76	0.83	0.82	0.57
Cu(2)	z	0.358 23(80)	0.359 54(50)	0.358 99(20)	0.359 54(20)	0.357 52(20)	0.355 81(20)
	B (in Å^2)	0.30	0.30	0.30	0.15	0.09	0.03
O(1)	n	0.225	0.201	0.248	0.350	0.817	0.999
O(2)	z	0.383 80(50)	0.381 89(30)	0.381 65(40)	0.380 89(60)	0.379 82(50)	0.379 24(40)
	B (in Å^2)	0.14	0.21	0.33	0.44	0.54	0.64
O(3)	z				0.379 20(40)	0.379 50(40)	0.379 41(30)
	B (in Å^2)				0.47	0.54	0.64
O(4)	z	0.160 77(120)	0.157 93(70)	0.157 70(30)	0.157 29(40)	0.159 59(40)	0.161 11(30)
	B (in Å^2)	2.01	1.50	1.71	1.55	1.19	0.46
R_p (%)		4.73	4.88	3.42	3.77	3.67	3.58
R_{wp} (%)		6.65	6.76	4.61	5.17	4.81	4.67
χ^2		12.2	10.8	5.31	4.59	4.31	4.38
Bond lengths	Yb-O(2)	2.3523(×8)	2.3662(×8)	2.3666(×8)	2.3728(×4)	2.3828(×4)	2.3864(×4)
	-O(3)				2.3726(×4)	2.3631(×4)	2.3577(×4)
	Ba/Sr-O(1)	3.0341(×0.225)	3.0173(×0.201)	3.0106(×0.248)	2.9525(×0.350)	2.9067(×0.817)	2.8587(×0.999)
	-O(2)	2.8819(×4)	2.8841(×4)	2.8819(×4)	2.9156(×2)	2.9433(×2)	2.9766(×2)
	-O(3)				2.8912(×2)	2.9221(×2)	2.9562(×2)
	-O(4)	2.7503(×4)	2.7527(×4)	2.7530(×4)	2.7415(×4)	2.7305(×4)	2.7198(×4)
	Cu(1)-O(1)	1.9167 (×2×0.225)	1.9171 (×2×0.201)	1.9177 (×2×0.248)	1.9233 (×2×0.350)	1.9292 (×2×0.817)	1.9308 (×2×0.999)
	-O(4)	1.8868(×2)	1.8546(×2)	1.8479(×2)	1.8351(×2)	1.8572(×2)	1.8711(×2)
	Cu(2)-O(2)	1.9400(×4)	1.9350(×4)	1.9360(×4)	1.9248(×2)	1.9196(×2)	1.9161(×2)
	-O(3)				1.9369(×2)	1.9461(×2)	1.9501(×2)
	-O(4)	2.3173(×1)	2.3676(×1)	2.3587(×1)	2.3597(×1)	2.3034(×1)	2.2613(×1)

the Yb$_2$BaCuO$_5$ impurity phase detected. Since the used FULLPROF Rietveld program allows simultaneous refinement of several phases, the neutron-diffraction data of the Cu(Ba$_{0.8}$Sr$_{0.2}$)$_2$YbCu$_2$O$_{6+z}$ samples were in preliminary refinements checked for the possible existence of the Yb$_2$BaCuO$_5$ phase. However, the contribution from the Yb$_2$BaCuO$_5$ structure[18] was found to be less than 1%, and consequently, in further refinements also the Cu(Ba$_{0.8}$Sr$_{0.2}$)$_2$YbCu$_2$O$_{6+z}$ samples were treated as single-phase materials. On the other hand, the solubility limit of calcium in Cu(Ba$_{0.8}$Sr$_{0.2}$)$_2$(Yb$_{1-x}$Ca$_x$)Cu$_2$O$_{6+z}$ is at $x = 0.35-0.40$, and in samples with $x > 0.35$ an increasing amount of BaCuO$_2$ impurity appears with increasing Ca concentration.[14] However, the present $x = 0.35$ sample was totally free from BaCuO$_2$ within the detection limits of XRD and NPD.

According to the results of several parallel coulometric titrations, post-annealing of the Cu(Ba$_{0.8}$Sr$_{0.2}$)$_2$(Yb$_{1-x}$Ca$_x$)Cu$_2$O$_{6+z}$ samples in Ar at 800 °C resulted in a slightly negative oxygen stoichiometry value z for some of the samples with $0 \leq x \leq 0.35$ (Table II). The negative values can be explained by a presence of trace amounts of an impurity phase of monovalent copper (Cu$_2$O). In order to obtain a reliable estimation for the oxygen excess z from the neutron-diffraction data as well, the isotropic temperature factor of the O(1) atom was fixed (at 0.3 Å^2) due to the very low occupancy of the site in the oxygen-deficient samples. The refinement of the O(1) occupancy in the samples annealed in Ar at 800 °C ended up to z values slightly decreasing with increasing Ca content x. In Table II, the values obtained by the two methods for the oxygen excess z in Ca-substituted samples are summarized, together with the observed T_c's. Corresponding data for the Ca-free samples, i.e., for the O-doped samples are presented in Table III. Even though the differences are quite small, the oxygen content values obtained from NPD refinements seem to be slightly higher than the coulometric titration results. In the following discussion of the efficiencies of the doping routes the z values refined from NPD data are assumed.

As the last steps of the NPD refinements, the partial occupancies of Yb and Ca at the R (i.e., Q) site and Ba and Sr at the A site were allowed to vary from the nominal values.
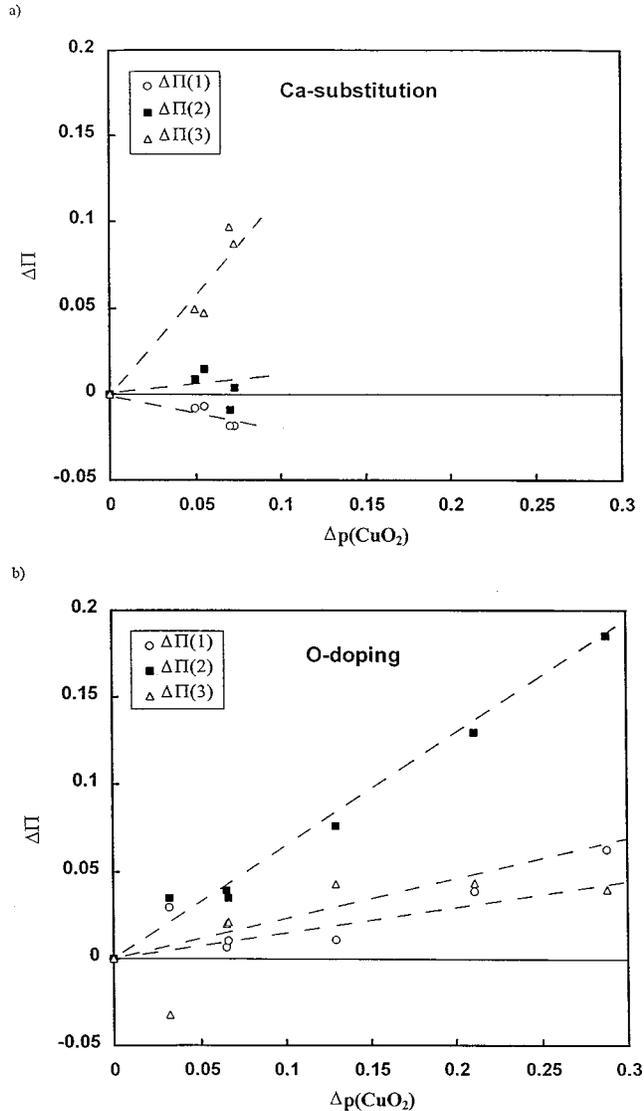
a)

b)

FIG. 3. Conductances of the different hole-doping routes in the $Cu(Ba_{0.8}Sr_{0.2})_2(Yb_{1-x}Ca_x)Cu_2O_{6+z}$ system: $\Delta\Pi$ (1,2,3) vs $\Delta p(CuO_2)$ for the (a) Ca-substituted ($z \approx 0$) and (b) O-doped ($x = 0$) samples.

However, since no improvements in the reliability factors were seen, the partial occupancies were fixed to the nominal values in the final refinements. The final results obtained from the refinements are shown in Tables IV and V. In general, the obtained R_p, R_{wp}, and χ^2 values are small, indicating a good reliability of the results.

In Ref. 14, the full series of Ca-substituted and O-doped $Cu(Ba_{0.8}Sr_{0.2})_2(Yb_{1-x}Ca_x)Cu_2O_{6+z}$ samples were characterized for the superconducting properties. In brief, without Ca substitution (i.e., $x=0$) the $Cu(Ba_{0.8}Sr_{0.2})_2YbCu_2O_{6+z}$ phase becomes superconducting when z exceeds 0.45. With increasing oxygen excess z, T_c increases in the same two-step manner as that commonly known for the $CuBa_2YCu_2O_{6+z}$ system. On the other hand, in the samples with $z \approx 0$, superconductivity appears at $x \approx 0.20$.

IV. DISCUSSION

Concerning the three possible hole-doping routes shown in Fig. 1, the hole produced in $Cu(Ba_{0.8}Sr_{0.2})_2(Yb_{1-x}Ca_x)$

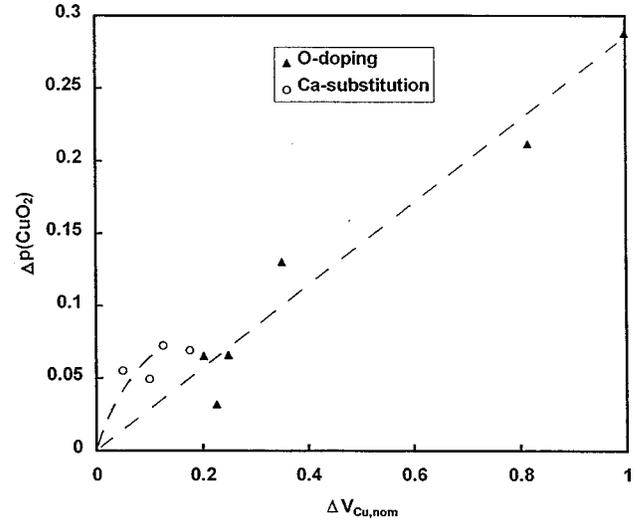FIG. 4. $\Delta p(CuO_2)$ vs $\Delta V_{Cu,nom}$ for the Ca-substituted ($z \approx 0$; $\bigcirc$) and O-doped ($x=0$; $\blacktriangle$) $Cu(Ba_{0.8}Sr_{0.2})_2(Yb_{1-x}Ca_x)Cu_2O_{6+z}$ samples.

Cu_2O_{6+z} by the excess oxygen are transferred into the CuO_2 plane for the most part via the gradual movements of the apical oxygen atoms towards the plane [route $\Pi(1)$] and barium atoms away from the in-plane oxygen atoms [route $\Pi(2)$], while doping with calcium substitution increases the hole concentration by lengthening the effective bond length, i.e., $R_{ij} - R_0$ in Eq. (5), from the in-plane oxygen to the (Yb,Ca) site [route $\Pi(3)$]. The contributions of the different routes with increasing doping levels, i.e., the $\Delta\Pi$ vs $\Delta p(CuO_2)$ curves, are illustrated in Figs. 3(a) and 3(b) for Ca substitution and O doping, respectively.

When considering the capability of the two different doping ways to generate holes into the CuO_2 plane, the hole concentration $p(CuO_2)$ as established by the bond-valence-sum calculation was found to increase less efficiently with O doping than with Ca substitution, as is seen in the $\Delta p(CuO_2)$ vs $\Delta V_{Cu,nom}$ correlations shown in Fig. 4. This is understand-

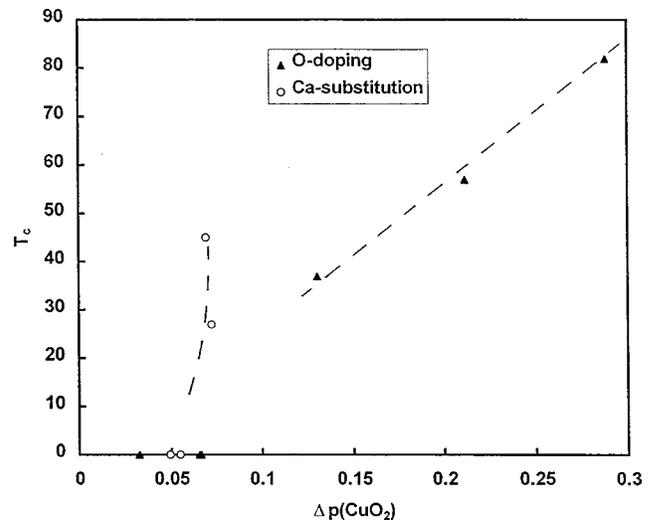FIG. 5. T_c vs $\Delta p(CuO_2)$ for the Ca-substituted ($z \approx 0$; $\bigcirc$) and O-doped ($x=0$; $\blacktriangle$) $Cu(Ba_{0.8}Sr_{0.2})_2(Yb_{1-x}Cu_x)Cu_2O_{6+z}$ samples.

able, since the excess oxygen atoms are located in the empty site around the chain-site Cu atoms, and are thus supposed to oxidize the CuO_z charge reservoir more efficiently. However, two less obvious observations were made from the data. Both of these observations are supported by our recent results obtained from O K-edge x-ray-absorption near-edge-structure measurements for the site-specific hole concentrations in the same sample powders.[19] First, not only O doping but also Ca substitution leads to smaller than nominal $\Delta p(CuO_2)$ values, i.e., $\Delta p(CuO_2) < \Delta V_{Cu,nom}$. This means that the Cu atoms in the charge-reservoir block are also partly oxidized with the Ca-to-Yb substitution. Since in the Ca-substituted samples practically no O atoms are present in the charge reservoir and the Cu atoms therefore are twofold coordinated, a mixed $+I/+II$ valence state is supposed for the partly oxidized chain-site Cu atoms. The second observation is that, the $\Delta p(CuO_2)$ values obtained for O-doped $Cu(Ba_{0.8}Sr_{0.2})_2YbCu_2O_{6+z}$ samples are quite large as compared to values calculated in the present way from NPD data reported for $CuBa_2YCu_2O_{6+z}$ (Refs. 6 and 7) $[\Delta p(CuO_2) = 0.15-0.20$ when z increases from ~ 0 to $\sim 1]$. It is noted that our preliminary measurements of the Seebeck coefficient for the $Cu(Ba_{0.2}Sr_{0.2})_2YbCu_2O_{6+z}$ samples indicated that with O doping overdoped state is reached at quite a low excess-oxygen value $(z \approx 0.8)$,[20] in accordance with the observed high $\Delta p(CuO_2)$ vs $\Delta V_{Cu,nom}$ rate.

When plotting the critical temperature as a function of the change in $p(CuO_2)$, i.e., against $\Delta p(CuO_2)$, it is seen (Fig. 5) that at a certain hole-concentration value higher T_c values are obtained with calcium substitution. The two different hole-doping ways also seem to result in different T_c vs (Cu-O bond length) relations [Fig. 6(a)]. In other words, increasing the hole concentration in the CuO_2 plane, i.e. the increase in $p(CuO_2)$, shortens the in-plane Cu-O bond length as a general trend since antibonding electrons are removed,[21] but the rate of shortening is different for the two hole-doping ways [Fig. 6(b)]. This suggests that other parameters besides the hole concentration have to be considered in terms of determining the superconducting properties. One possible additional parameter is the hole distribution in the in-plane Cu-O bond. That is, whether the holes have more $Cu(3d)$ or $O(2p)$ character. In that respect, note that the $Cu(+III)$-$O(-II))$ and $Cu(+II)$-$O(-I)$ bonds have different characteristic lengths, i.e., $R_0[Cu(+III)-O(-II)] \approx 1.73$ and $R_0[Cu(+II)-O(-I)] \approx 1.59$.[9] Therefore, according to a bond-valence interpretation, within a certain amount of net holes being accomodated in the Cu-O bond, i.e., s_{ij} is fixed, the shorter the R_{ij} value is, the smaller the R_0 should be [cf. Eq. (5)], and consequently the more the holes would be on oxygen.[3,22]

Another factor which also may affect the T_c value is the buckling of the CuO_2 planes. From the (flatness of the CuO_2 plane) vs $\Delta \Pi(1)$ data summarized for the both hole-doping ways in Fig. 7 it can be concluded that the more the holes are doped via $\Pi(1)$ the stronger is the buckling of the CuO_2 planes. The fact that, at a certain $p(CuO_2)$ value a lower T_c value is obtained when the increase in $p(CuO_2)$ is achieved via $\Pi(1)$, is consistent with the observation of Jorgensen *et al.*[23] that among the different cuprate phases the highest T_c values can be assigned to the structures with the longest Cu-O_{api} distances. An interesting question is, whether this
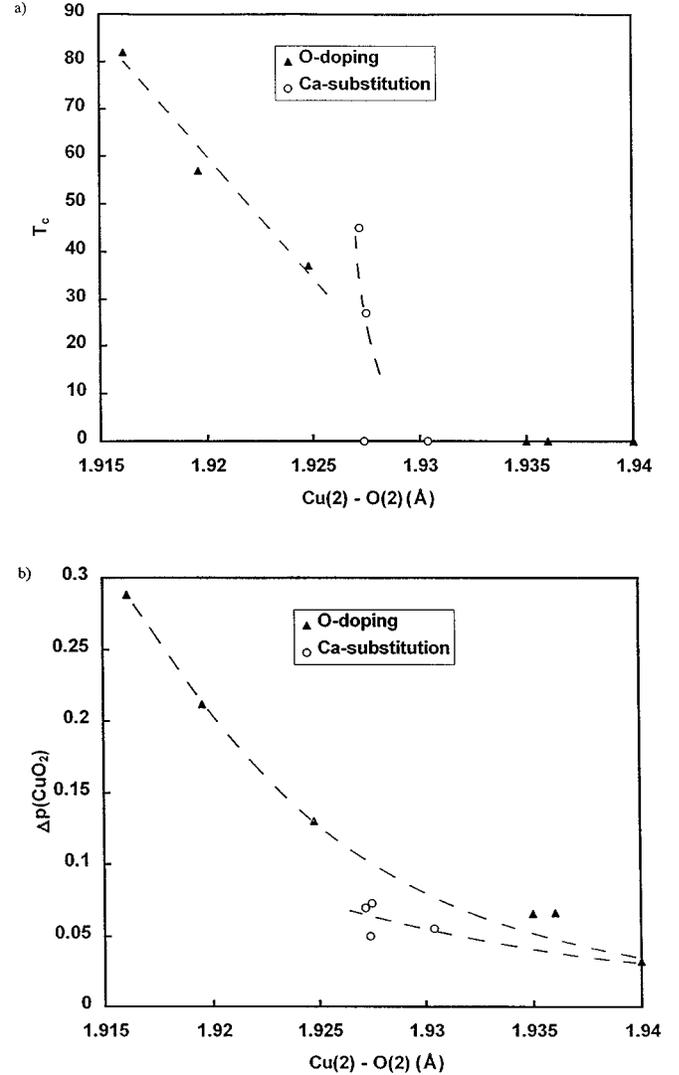

FIG. 6. (a) T_c and (b) $\Delta p(CuO_2)$ vs Cu(2)-O(2) bond length for the Ca-substituted $(z \approx 0; \ \bigcirc)$ and O-doped $(x=0; \ \blacktriangle)$ $Cu(1)(Ba_{0.8}Sr_{0.2})_2(Yb_{1-x}Ca_x)Cu(2)_2O_{6+z}$ samples.

interpretation can be extended to square-planar CuO_2 planes, e.g., the inner CuO_2 planes in the $M_mA_2Q_{n-1}Cu_nO_{m+2+2n\pm\delta}$ phases with $n \geq 3$, in which the Cu-O_{api} distance can be thought to be infinite.[3,22]

V. CONCLUSIONS

In the present study, the distinct calcium-substitution and oxygen-doping effects were established in the $Cu(Ba_{0.8}Sr_{0.2})_2(Yb_{1-x}Ca_x)Cu_2O_{6+z}$ system. The two different hole-doping ways were found to exhibit different T_c vs $p(CuO_2)$ and (Cu-O bond length) vs $p(CuO_2)$ characteristics. Also, calcium substitution diminished the buckling of the CuO_2 plane while oxygen doping increased the buckling. In an $M_mA_2Q_{n-1}Cu_nO_{m+2+2n\pm\delta}$ system in general, the hole concentration $p(CuO_2)$ in the (CuO_2) planes is determined as a delicate balance within the exact oxygen content δ and the nature (valence and size) of the cations M, A, and Q, and the results obtained for the $Cu(Ba_{0.8}Sr_{0.2})_2(Yb_{1-x}Ca_x)Cu_2O_{6+z}$ system cannot be directly adapted to each different combination of δ, M, A, and Q even at a fixed n. However,
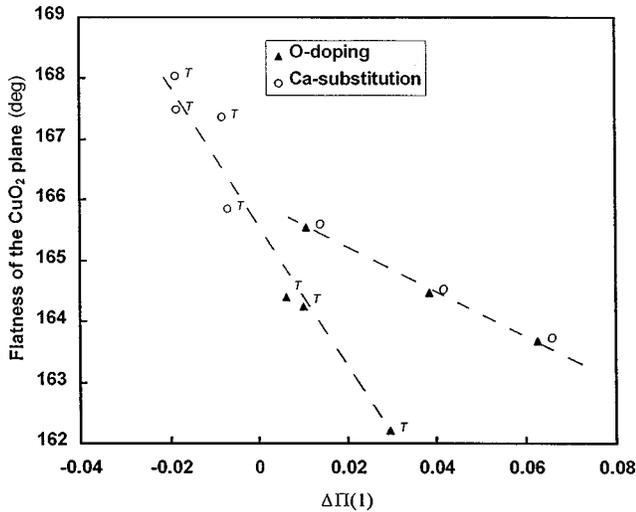
FIG. 7. (Flatness of the CuO_2 plane) vs $\Delta\Pi(1)$ for the Ca-substituted ($z \approx 0$; $\bigcirc$) and O-doped ($x=0$; $\triangle$) $Cu(Ba_{0.8}Sr_{0.2})_2(Yb_{1-x}Ca_x)Cu_2O_{6+z}$ samples. Tetragonal and orthorhombic samples are indicated by T and O, respectively.

as a general conclusion the present study demonstrated that, not only the hole concentration but also other parameters such as the hole distribution among the Cu and O atoms and the degree of buckling are important in determining the superconducting properties of the CuO_2 planes. We believe that considering the distinct contributions of the different hole-doping routes is essential for understanding the superconducting cuprate materials and to be able to explain why, e.g., $T_{c,\text{optimized}}$ varies from one cuprate phase to another. Also, in terms of improving the irreversibility field (H_{irr}) properties, possibility to control the hole distribution between the infinite-layer and charge-reservoir blocks by guiding the holes in the desired part of the layered cuprate structure would be most attractive.[24,25]

ACKNOWLEDGMENTS

[1] H. Yamauchi, M. Karppinen, and S. Tanaka, Physica C **263**, 146 (1996).

[2] M. Karppinen and H. Yamauchi, J. Supercond. **11**, 39 (1998).

[3] M. Karppinen and H. Yamauchi, Philos. Mag. B **79**, 343 (1999).

[4] I. D. Brown and D. Altermatt, Acta Crystallogr., Sect. B: Struct. Sci. **41**, 244 (1985).

[5] I. D. Brown, J. Solid State Chem. **82**, 122 (1989).

[6] R. J. Cava, A. W. Hewat, E. A. Hewat, B. Batlogg, M. Marezio, K. M. Rabe, J. J. Krajewski, W. F. Peck, Jr., and L. W. Rupp, Jr., Physica C **165**, 419 (1990).

[7] J. D. Jorgensen, B. W. Veal, A. P. Paulikas, L. J. Nowicki, G. W. Grabtree, H. Claus, and W. K. Kwok, Phys. Rev. B **41**, 1863 (1990).

[8] J. L. Tallon, Physica C **168**, 85 (1990).

[9] I. D. Brown, Physica C **169**, 105 (1990).

[10] Based on the nomenclature given in Fig. 2 and in Eqs. (5)–(7):

$$p(CuO_2) = V_{Cu(2)} + V_{O(2)} + V_{O(3)} + 2$$

$$= s_{Cu(2)\text{-}O(4)} + 2s_{Cu(2)\text{-}O(2)} + 2s_{Cu(2)\text{-}O(3)} - 2s_{Cu(2)\text{-}O(2)}$$

$$- 2s_{Cu(2)\text{-}O(3)} - 2s_{A\text{-}O(2)} - 2s_{A\text{-}O(3)}$$

$$- 2s_{Q\text{-}O(2)} - 2s_{Q\text{-}O(3)} + 2$$

$$= s_{Cu(2)\text{-}O(4)} - 2s_{A\text{-}O(2)} - 2s_{A\text{-}O(3)} - 2s_{Q\text{-}O(2)}$$

$$- 2s_{Q\text{-}O(3)} + 2.$$

[11] P. Berastegui, S.-G. Eriksson, L. G. Johansson, M. Kakihana, M. Osada, H. Mazaki, and S. Tochihara, J. Solid State Chem. **127**, 56 (1996).

[12] G. Böttger, I. Mangelschots, E. Kaldis, P. Fischer, Ch. Krüger, and F. Fauth, J. Phys.: Condens. Matter **8**, 8889 (1996).

[13] V. P. S. Awana, S. K. Malik, and W. B. Yelon, Physica C **262**, 272 (1996).

[14] K. Fujinami, M. Karppinen, and H. Yamauchi, Physica C **300**, 17 (1998).

[15] M. Karppinen, A. Fukuoka, L. Niinistö, and H. Yamauchi, Supercond. Sci. Technol. **9**, 121 (1996).

[16] K. Kurusu, H. Takami, and K. Shintomi, Analyst (Cambridge, U.K.) **114**, 1341 (1989).

[17] J. Rodriguez-Carvajal, Physica B **192**, 55 (1993).

[18] P. Lightfoot, S. Pei, J. D. Jorgensen, Y. C. Chang, P. Z. Jiang, and B. W. Veal, J. Solid State Chem. **89**, 385 (1990).

[19] M. Karppinen, H. Yamauchi, T. Nakane, K. Fujinami, K. Peitola, P. Nachimuthu, R.-S. Liu, and J. M. Chen (unpublished).

[20] T. Nakane, K. Isawa, M. Karppinen, and H. Yamauchi (unpublished).

[21] J. B. Goodenough, Supercond. Sci. Technol. **3**, 26 (1990).

[22] H. Yamauchi and M. Karppinen, J. Supercond. **11**, 43 (1998).

[23] J. D. Jorgensen, O. Chmaissem, D. G. Hinks, A. Knizhnik, Y. Eckstein, H. Shaked, J. L. Wagner, B. Dabrovski, S. Short, J. F. Mitchell, and J. P. Hodges, in *High-Temperature Superconductors and Novel Inorganic Materials*, Vol. 62 of *NATO Advanced Study Institute, Series 3: High Technology*, edited by G. Van Tendeloo, E. V. Antipov, and S. N. Putilin (Kluwer, Dordrecht, 1999), pp. 109–116.

[24] H. Yamauchi, M. Karppinen, K. Fujinami, T. Ito, H. Suematsu, K. Matsuura, and K. Isawa, Supercond. Sci. Technol. **11**, 1006 (1998).

[25] T. Nakane, K. Fujinami, M. Karppinen, and H. Yamauchi, Supercond. Sci. Technol. **12**, 242 (1999).